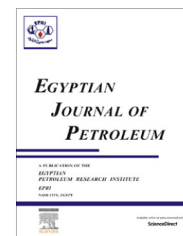




Egyptian Petroleum Research Institute
Egyptian Journal of Petroleum

www.elsevier.com/locate/egyjp
www.sciencedirect.com



FULL LENGTH ARTICLE

Rice husk templated water treatment sludge as low cost dye and metal adsorbent

Nasser H. Shalaby^{a,*}, Emad M.M. Ewais^b, Riyad M. Elsaadany^c, Adel Ahmed^c

^a Egyptian Petroleum Research Institute, Nasr City, 11727 Cairo, Egypt

^b Refractory & Ceramic Materials Division (RCMD), Central Metallurgical R&D Institute (CMRDI), P.O. Box 87 Helwan, 11421 Cairo, Egypt

^c Inorganic Chemistry, Faculty of Science, Helwan University, Helwan, Egypt

Received 12 May 2016; revised 18 September 2016; accepted 12 October 2016

KEYWORDS

Adsorption;
 Water treatment sludge;
 Rice husk;
 Mesoporous adsorbents

Abstract The preparation of adsorbents at low cost as alternatives to the expensive ones in the treatment processes of water and wastewater is the interest of the researchers worldwide. Here, a novel cheap mesoporous adsorbent was prepared via the recycling of wastes namely water treatment sludge and rice husk (RH) as textural modifier. Surface area and pore dimensions were optimized against RH ratio. The mesoporous sludge was employed in adsorption of rosaniline dye, Pb²⁺, Ni²⁺ and chlorine from aqueous solutions under dynamic experimental conditions. It was found that the initial dye concentration and textural structure of the adsorbent played important roles in adsorption capacity. The reusability test shows the ease desorption of dye with slightly alkaline water (pH = 8) indicating the stability and reusability of the ceramic adsorbent for several times. For metallic cations, the characteristics (ionic radius and ΔH_{hyd}) of ions affect the adsorption affinity. Chlorine adsorption is controlled by the cation exchange capacity (CEC).

© 2016 Egyptian Petroleum Research Institute. Production and hosting by Elsevier B.V. This is an open access article under the CC BY-NC-ND license (<http://creativecommons.org/licenses/by-nc-nd/4.0/>).

1. Introduction

During the last decades, the exponential population and social civilization expansions, changes in the habits of life and resources used coupled with continuing progress of the industrial and technologies have led to a sharp modernization and metropolitan growth [1]. With the growing awareness of the occurrences of industrial activities, many alterations on several ecosystems have been intensified and began to seriously threaten

human health and the environment. Among the many cases of pollution of the aqueous medium, the contamination of water by dyes and heavy metals when a wide range of chemical products and dyes are discharged directly or indirectly in the course of the water without adequate treatment to remove and degrade these harmful compounds. More than 100,000 commercially available dyes are known and approximately 1 million tons of these dyes are produced annually worldwide. The main sources of dye contamination are considered to be from textile industry [2].

Wastewater from the textile industry is a complex mixture of many polluting substances ranging from residual dyestuffs to heavy metals associated with the dyeing and printing processes. Wastewater from processes of reactive dye is particu-

* Corresponding author. Fax: +20 222747433.

E-mail address: chem.shalaby@gmail.com (N.H. Shalaby).

Peer review under responsibility of Egyptian Petroleum Research Institute.

<http://dx.doi.org/10.1016/j.ejpe.2016.10.006>

1110-0621 © 2016 Egyptian Petroleum Research Institute. Production and hosting by Elsevier B.V.

This is an open access article under the CC BY-NC-ND license (<http://creativecommons.org/licenses/by-nc-nd/4.0/>).

larly problematic because these dyes have low levels of attachment to the fibers. 30% or more of the dyes used are hydrolyzed and then released into waterways. The brightly colored unfixed dyes are highly water soluble, have poor adsorption properties and are not removed by conventional treatment systems. Although these dyes are not in themselves toxic, they may be converted into potentially carcinogenic amines after release into the aquatic environment. Their disposal is always a matter of great concern because they are considered as a whole in fact dangerous source of pollution of the environment and may result in the direct destruction of aquatic life due to the presence of chlorides of metals and aromatics which interferes with the penetration of the light and the oxygen in water bodies leading to a conflict between the upstream discharger and downstream user water.

Various techniques [3–6] have been developed for the removal of dyes and heavy metals from wastewater. Among them, adsorption is an especially effective approach. The adsorbents at low cost for the air/water purification have much attracted the attention of researchers around the world. One of these cheap materials is the water treatment sludge (WTS) produced during the pre-treatment of Nile water before demineralization as a feed-water for boilers at power stations and at the domestic water treatment plants. The composition and properties of WTS depends on the quality of the raw water, and the type of chemical treatment used in the treatment processes. The recycling of sludge from water treatment plants is usually an attempt to reduce its volume, make it harmless and stable, retrieve and facilitate its content useful safe disposal without imposing a burden for the environment [7,8]. The sludge contains mainly a high concentration of salts of aluminum or iron, with a mixture of organic and inorganic materials and the precipitates of hydroxide [7].

Adsorption of large molecules (e.g. drug delivery, biomedical application, dyes, purification of biofluids, water purification technologies) requires the design of new porous materials with extended pore diameter in the mesoporous range (pore dimensions above 2 nm) [9–11]. Mesopores constitute the pathways for large molecules to access the inner porous structure (primary adsorption sites), thus improving the adsorption kinetics.

On the other hand, large quantities of crop residues in term of rice husk (RH) are produced annually worldwide, and are vastly underutilized. Since Egypt's rice plantation is among the highest in the world, 4.0 million tons of wastes are left behind annually. Some residues are used to feed animals or recycled, yet open burning remains the most widespread technique of disposal. Such practice, which is only one of many other open burning activities, deteriorates air quality of Cairo and the Delta governorates contributing to the black cloud phenomenon, acts as the potential risk of developing serious health problems (due to the emission of carbon monoxide and other toxic emissions) and consequently, poses potential economic threats. Therefore, it is necessary to find a suitable method to solve the disposal problem. Using of this cheap material as a natural organic template in modification and improvement of textural structure of water treatment sludge as ceramic adsorbent, contributes to the solution of this problem and achieve the principle "waste-waste self-cleaning".

This work aims at developing of porous material from RH and water treatment sludge as low cost dyes and metals adsorbent.

2. Experimental

2.1. Materials

The raw sludge used in this study was sourced from the water treatment plant at El-Kureimat power station (Giza, Egypt), rice husk (RH) is provided by the rice mills at Cairo, Egypt. All chemicals used (rosaniline dye, $\text{Pb}(\text{NO}_3)_2$ and $\text{Ni}(\text{NO}_3)_2 \cdot 6\text{H}_2\text{O}$) are analytical grades and purchased from Prolabo. Stock solutions of the dye at concentrations of 1.48×10^{-4} mol/L, 8.88×10^{-5} mol/L and 4.44×10^{-5} mol/L were prepared. The solutions of Pb^{2+} and Ni^{2+} were prepared at concentrations of 1.7×10^{-4} mol/L. A sample of water contaminated with residual chlorine of concentration 1.41×10^{-5} mol (1 ppm) was drownd from the pretreatment cycle of demineralizer feed water at Upper Egypt Electricity Production Company (UEEPC).

2.2. Preparation of mesoporous sludge

5, 10 and 15% wt.% rice husk were well-mixed with raw sludge (RS) to ensure homogeneity of the mixture. The mixed pastes were molded in wood mold and left to dry away from the sun for seven days. After that, the samples were dried at 95 °C for 24 h then were fired in a temperature programming muffle furnace (Nabertherm 330 P, Germany) at 900 °C for 3 h with a heating rate of 5 °C/min. The prepared samples were denoted as RS-RH5%, RS-RH10% and RS-RH15%, respectively.

2.3. Testing procedures

Nitrogen adsorption/desorption isotherms were performed to characterize the texture of the calcined samples at 900 °C. Nitrogen adsorption and desorption isotherms at -196 °C of the calcined samples were collected at 77 K using a Quantachrome Autosorb-1C apparatus. Prior to the measurements, the samples were degassed in vacuum at 250 °C for 3 h. Specific surface areas (SSA) of these samples were calculated using the Brunauer-Emmett-Teller (BET) equation ($p/p_0 = 0.05-0.15$). The total pore volume was determined at relative pressure $p/p_0 = 0.98$. The pore size distribution was estimated according to the quenched solid density functional theory (QSDFT) equilibrium model for slit pores using the Autosorb 1.56 software from Quantachrome. The micropore volume and surface area were also calculated by the above mentioned DFT model.

XRD analysis of the calcined raw sludge was performed by X-ray diffractometer, PANalytical model X_{per} PRO, equipped with a Cu K α radiation ($\lambda = 1.5418 \text{ \AA}$) at scanning rate of $0.3^\circ \text{ min}^{-1}$. Structural characteristics of the sorbent samples were studied via FTIR analysis, using ATI Mattson WI, 53717 model Genesis spectrometer, USA. The metal content of rice husk ash (RHA) and the cation exchange capacity (CEC) of the obtained mesoporous sludge were determined at Desert Research Center, El Matariya, Cairo. The metal content was determined using Inductively Coupled Argon Plasma, iCAP 6500 Duo, Thermo Scientific, England standardized with 100 mg/L multi-element certified solution, Merck, Germany. The CEC was determined using sodium acetate method which was found 12.5 mEq/100 g. Chemical analysis of sludge was

determined by analytical XRF (Model advanced Axios, Netherlands). 1 g of the sample was fired at 1000 °C for 2 h to calculate the loss on ignition, and then 10 g of the sample was pressed with 2 g wax as a binder in an aluminum cup, and then exposed to X-rays as a disk. The acidic characters of the mesoporous sludge was investigated by temperature programmed desorption of ammonia with dynamic flow method and thermal conductivity detector (W-Re filament), BEL-CAT-B, Japan. The adsorption performance of texturally modified sludge was achieved at room temperature using continuous flow adsorption experiment conducted in a fixed bed glass column with an inner diameter of 1.2 cm, a height of 20 cm and a medium porosity sintered-Pyrex disk at its bottom in order to prevent any loss of material, Fig 1. A bed depth of 5.8 cm (6.0–6.5 g) was investigated at a constant flow rate of 4 mL/min using scaled dropping funnel. Before being used in the experiments, approximately 100 ml of demineralized water were passed through the column to remove any non consolidated and fine particles and to verify the absence of soluble species. The dye solution was then poured at the top of the column and allow to flow along the column by gravity.

The samples of effluent leaving the bottom of the adsorption column were collected at different time intervals and analyzed for adsorbate determination. Total organic carbon (TOC) in rosaniline dye effluent was determined as a function in dye concentration using analytikjena Multi N/C 2100s, Germany. The effluent of lead and nickel salts was analyzed for Pb^{2+} and Ni^{2+} determination using flame atomic absorption spectrometer ZEE nitu 700P-analytik Jena – Germany. Chlorine was determined using DPD free chlorine reagent (25 ml sample /cat 14070-99) test kit HACH Company world Headquarters USA. Chlorides in influent and effluent were estimated using 0.0141N standard silver nitrate solution, HACH, USA. Area under breakthrough curves was calculated using Origin 5 program.

3. Results and discussion

3.1. BET - textural investigation

N_2 adsorption-desorption pore size distribution curves (PSD) are shown in Fig. 2. The specific surface area ($S_{BET} m^2/g$) and pore dimensions of the different samples are summarized in Table 1. The increased surface area of rice husk modified sludge samples, viz., RS-RH5%, RS-RH10% and RS-RH15% is mainly attributed to the combustion of rice husk organic components leaving several pores, the dimensions (average pore radii, r_p nm and pore volume, V_p cm^3/g) of which are controlled by concentration and homogeneity of rice husk fiber distribution. With increasing the rice husk content, narrower pores are obtained where the residual ash occupies a large space of created pores volume causing the reduction of created surface area. The pore size distribution curve (PSD) of RS shows poly-modal pore size distribution curves with many ranges of pore radii. The first, second, third and fourth ranges are interconnected with narrow pores starting from 7.7 Å to 21.3 Å while the fifth and sixth ranges are the main, larger and interconnected with wider pores from 21.3 Å to 56.8 Å.

From the obtained data in Table 1, RS-RH5% and RS-RH15% were selected to be candidates as sorbents for waste water treatment. The selected samples were used for removal of rosaniline dye, residual chlorine, Pb^{2+} and Ni^{2+} . These pollutants were chosen for our study because they are common in waste water. Continuous flow adsorption experiments were conducted in a fixed-bed glass column with the concept of the breakthrough curve to emulate the industrial applications.

3.2. XRD analysis

XRD patterns of the raw sludge (just dried at 105 °C) and calcined sludge at 900 °C are shown in Fig. 3. Ignition of the sample at 900 °C suppresses the interference of peaks of clay with quartz, increases the relative intensity of the peaks of quartz and reduces the initial matrix variation of samples which fits with the elemental analysis of two samples [12]. In Fig. 3, the narrow and sharp peaks indicate that the samples possess a high crystallinity with high surface charge density which enhances the electrostatic attraction with the adsorbate molecules [13].

From the diffraction data, mainly quartz and illite could be identified. Quartz is identified by its 3.34 Å and 4.26 Å spacing (2θ , 20.85–26.69°). Illite is identified by d -spacing 9.9–10 Å (2θ , 8.93–8.84°) and 4.5–5 Å (2θ , 19.73–17.74°) and 1.542–1.004 Å (2θ , 30–50.16°) (see Tables 2–4).

3.3. Temperature programmed desorption of ammonia (TPD-ammonia)

Fig. 4 depicts the TPD- NH_3 profile of RS-RH5%. It can be seen from Fig. 4 that desorption of ammonia from the sample

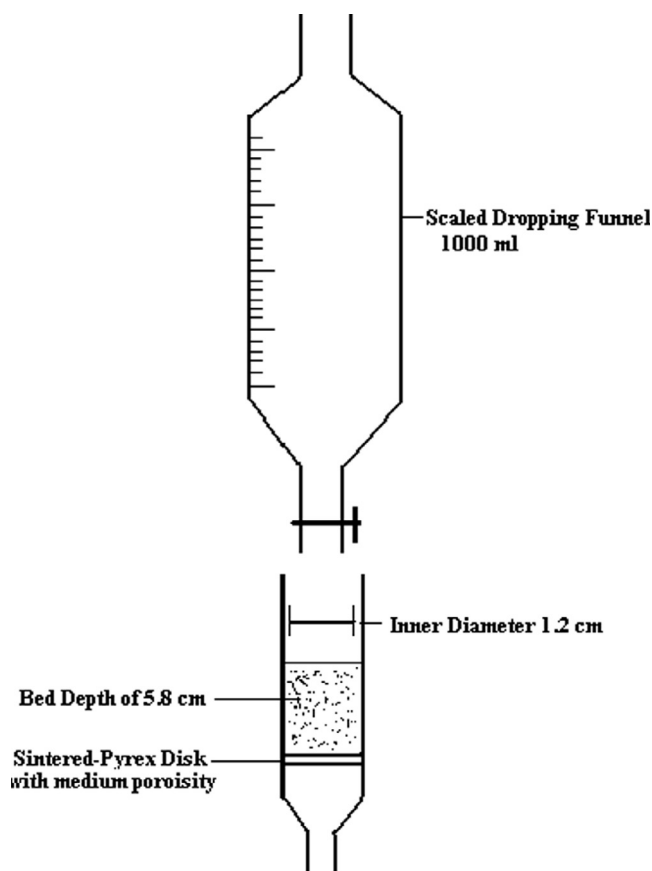


Figure 1 Schematic diagram of the fixed-bed adsorption column.

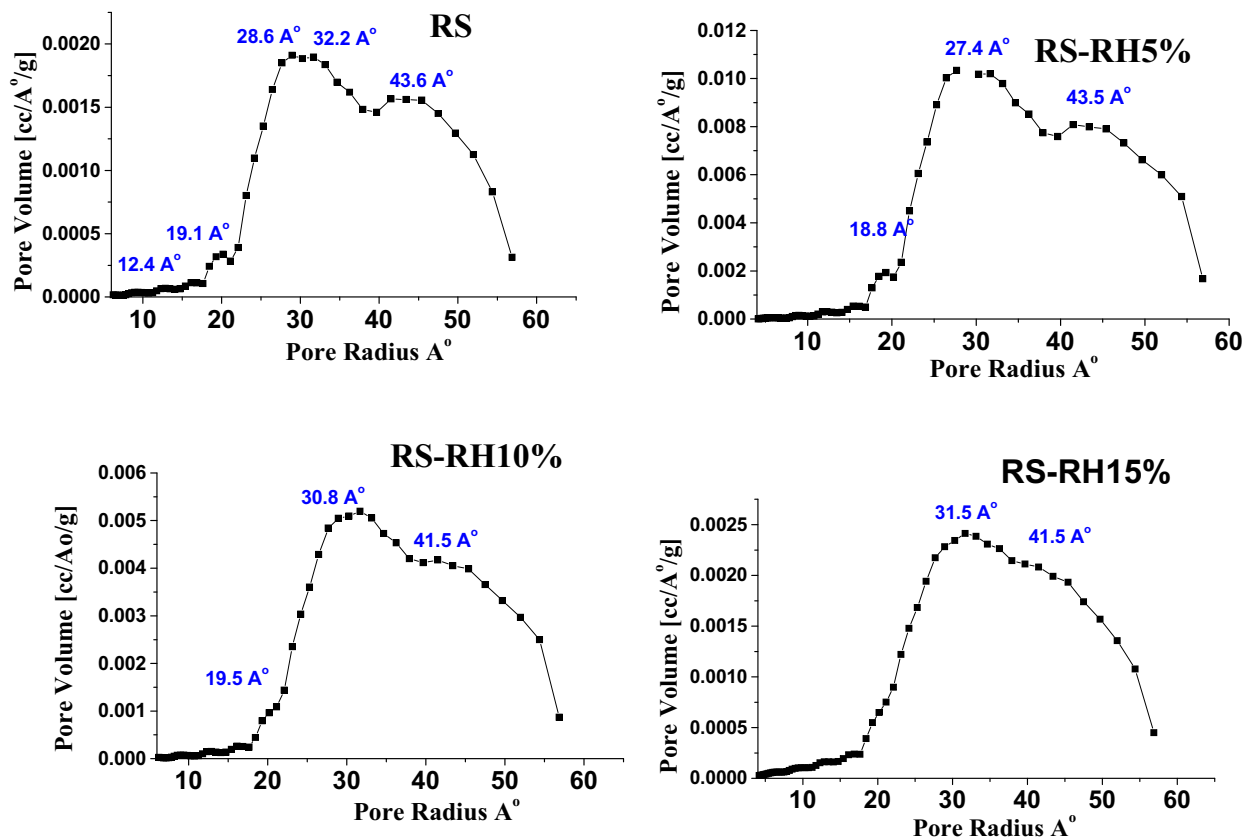


Figure 2 Barrett-Joyner-Halenda (BJH) pore size distribution curve of RS, RS-RH5%, RS-RH10% and RS-RH15%.

Table 1 BET surface area and pore dimensions of raw sludge (RS), RS-RH5%, RS-RH10 and RS-RH15% (calcined at 900 °C).

Sample	S_{BET} (m ² /g)	r_p (nm)	V_p (cm ³ /g)
Raw Sludge (RS)	62.94	1.84	0.0511
RS-RH5%	341.2	3.2	0.2714
RS-RH10%	182.2	2.8	0.1320
RS-RH15%	94.25	2.1	0.0679

starts at 100 °C and reaches its maximum at temperatures of about 370 °C. The profile shows two isolated peaks of ammonia desorption referring to different strength of two acidic sites on the surface. The first peak is centered at 160 °C corresponding to the weak acid sites, while the second peak is centered at 370 °C and corresponding to the strong acid sites is usually attributed to the ammonia desorption from the Brønsted acid sites [14]. The amount of acid sites on the clay surface was estimated by integration of the NH₃ desorption peaks and was found to be 59.7 μmol/g.

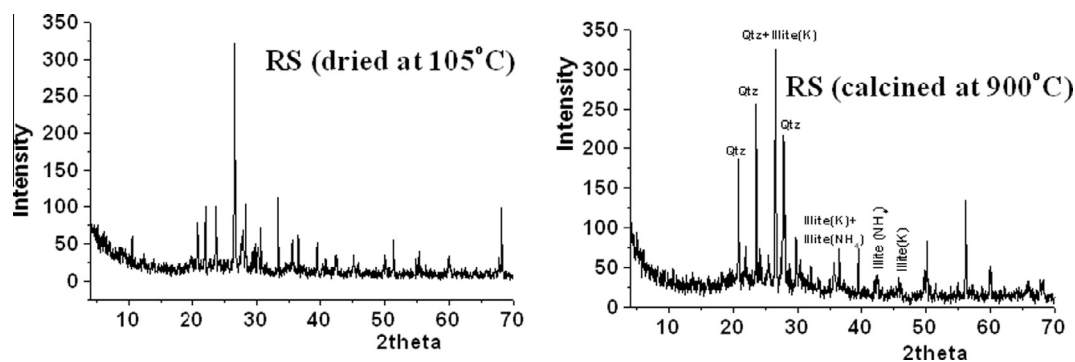


Figure 3 XRD patterns of RS.

Table 2 XRD data of RS (calcined at 900 °C).

2θ	20.8	21.9	23.6	26.6	27.8	28.0	29.8	36.3	39.4	42.4	50.0	56.1	59.9	65.9	67.9
D (Å)	4.3	4.0	3.8	3.4	3.2	3.2	3.0	2.5	2.3	2.1	1.8	1.6	1.5	1.4	1.4

Table 3 Chemical analysis RS.

Chemical constituent	SiO ₂	Fe ₂ O ₃	Al ₂ O ₃	CaO	MgO	TiO ₂	SO ₃	Na ₂ O	K ₂ O	P ₂ O ₅	MnO	Ignition loss
wt. %	<i>RS (just dried at 105 °C)</i>											
	34.43	8.203	16.549	4.539	0.716	0.920	2.572	0.212	0.416	0.726	0.150	30.2
	<i>RS (calcined at 900 °C)</i>											
	49.822	11.823	23.854	6.497	1.053	1.34	3.63	0.308	0.505	0.95	0.218	–

Table 4 The mineral content (wt.%) of RHA.

Sample	Al ₂ O ₃	K ₂ O	CaO	MgO	MnO ₂	Fe ₂ O ₃	ZnO
RHA	0.15	0.65	0.68	0.62	0.1	0.23	0.01

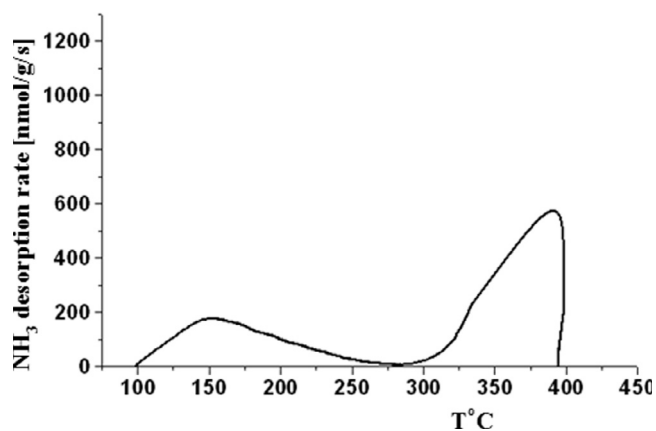
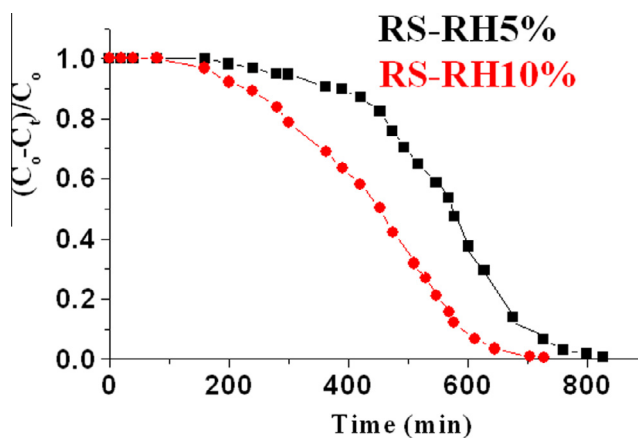
3.4. Adsorption performance of modified sludge

3.4.1. Dye-adsorption

The effectiveness of modified sludge in the removal of rosaniline dye was evaluated under dynamic conditions using a fixed-bed column (as indicated in the experimental section). The rosaniline dye initial concentration in the column influent (C_o) was varied from 1.48×10^{-4} mol/L (50 ppm), 8.88×10^{-5} mol/L (30 ppm) to 4.44×10^{-5} mol/L (15 ppm). In all experiments, flow to the column continued until the effluent dye concentration at time t (C_t) reached the influent dye concentration (C_o): $C_t/C_o \approx 1$. Fig. 5 depicts the results graphically at influent concentration of 1.48×10^{-4} mol/L (50 ppm). For a constant flow rate and at a given influent dye concentration the total quantity of dye retained in the column (Q total in μmol) was obtained graphically by numerically integrating the area under the curve $(C_o - C_t)/C_o$ vs. service time (as shown in Fig. 5) [15]. The highest Q_{total} value obtained was for the sorption of 561.29655 μmol (0.18964 g) at $C_o = 50$ ppm onto RS-

RH5% surface, Fig. 6. At the same concentration ($C_o = 50$ ppm), the sorbed amount onto RS-RH10% surface was 426.021 μmol (0.14394 g) which runs in harmony with the textural analysis of each sorbent, Table 1. It was noted that the adsorbed dye is easily eluted with slightly alkaline water without change in its original color indicating the dye molecules are mainly physisorbed.

Concentration of initial dye seems to have an impact on the sorption process such as the increase in the initial concentration of dye solution, the adsorption of the dye is higher [16]. It is because to lower the initial concentration, the ratio of the initial number of moles of dyes for the available surface area is low. In addition, the initial concentration of the dye molecules in the solution plays a key role as a driving force to overcome the resistance of mass transfer between the aqueous and solid phases [17]. At the beginning, most of the solute is adsorbed because it is exposed to the fresh sorbent and therefore, concentrations near zero would be provided at the level of the output of the column.

**Figure 4** Profiles of TPD-ammonia for RS-RH5%.**Figure 5** Breakthrough curves for rosaniline dye at influent concentration of 50 ppm.

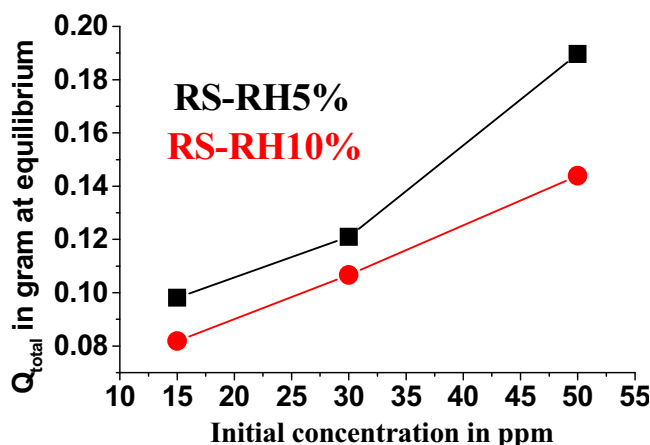


Figure 6 Dye removal with variation of initial dye concentration at constant dosages of adsorbent.

Fig. 7 shows IR spectra for RS-RH5%, rosaniline dye (RD) and adsorbed dye onto the modified sludge surface (RS-RH5%-RD). The spectrum of RS-RH5% shows a strong band around 3444 cm^{-1} which indicates the hydrogen bonding interactions associated with available silanols (of clay surface and rice husk ash) and the presence of physisorbed water on the sludge surface [18]. The band around 1635 cm^{-1} can be attributed to the bending vibration of water molecules bound to the silica matrix [19]. The broad band at 1085 cm^{-1} is attributed to the stretching of Si—O—Si of silica. The band near 938 cm^{-1} due to $\text{H—O}\cdots\text{Fe}^{3+}$ is absent, indicating that the iron is mainly present as oxide. The band around 800 cm^{-1} represents OH groups bound to one iron and one aluminum or magnesium neighbor [20]. The spectrum of the rosaniline dye depicts the absorption peaks of its characteristic functional groups. Spectrum shows a peak at 1140 cm^{-1} corresponding to the C—N stretching vibrations, a peak at 1590 cm^{-1} corresponding to the C=C stretching of the benzene ring and a peak at 2910 cm^{-1} for C—H stretching of asymmetric CH_3 group [21].

The spectrum of the adsorbed dye (RS-RH5%-RD) shows the disappearance of peaks characteristic the dye spectrum except the weak peaks of C—H stretching of asymmetric

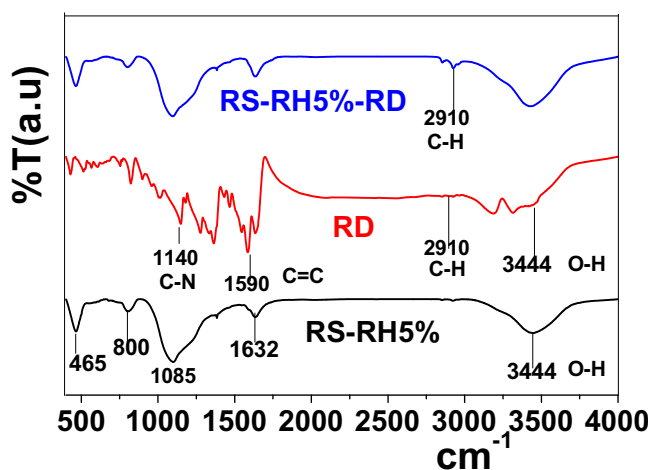


Figure 7 IR spectra of RS-RH5%, RD and RS-RH5%-RD.

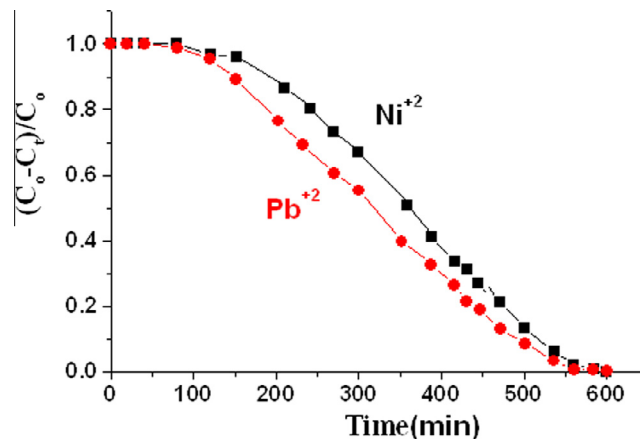


Figure 8 Breakthrough curves for Ni(II) and Pb(II) at influent concentration of $1.7 \times 10^{-4}\text{ mol/L}$ onto RS-RH5% surface.

CH_3 group. This attributed to the strong adsorption of the functional groups of dye molecules (due to the electrostatic force between adsorbent surface charge, NH_2 and benzene rings) which restrict the bond vibration and IR absorption. But in the case of CH_3 group, its adsorption is only under the effect of van der Waals forces [22].

3.4.2. Periodicity test

After the exhaustion of the adsorbent column containing RS-RH5%-RD at different initial concentrations, the reusability of the adsorbent was studied in each experiment by unpacking the glass column into a beaker containing 1 L of slightly alkaline distilled water ($\text{pH} = 8$) and was magnetically stirred for 2 h. The adsorbent was separated by filtration and the amount of desorbed dye was calculated by the TOC determination. The amount of desorbed dye at $C_o = 15\text{ ppm}$, 30 ppm and 50 ppm was 61.41%, 68.67% and 80.1% from the adsorbed amount respectively. The alkaline medium weakens the electrostatic interaction between the acid sites of the adsorbent and the NH_2 groups of the dye molecules [23]. On the other hand, the incomplete desorption of the dye may be attributed to the dual process of physisorption and chemisorption [23]. In the second period, the exploited adsorbent (RS-RH5%)_{Re} maintained about 91.2% of adsorption capacity against the

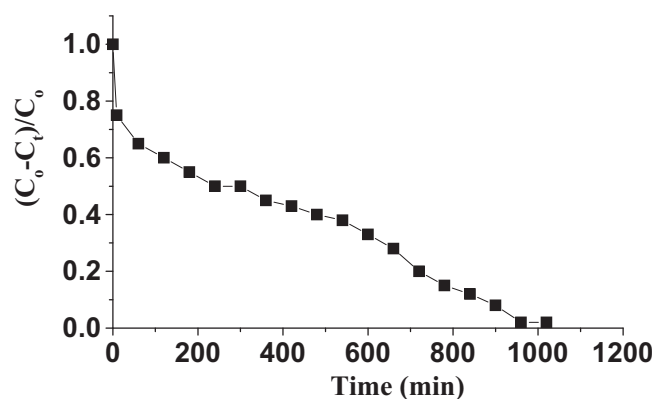


Figure 9 Breakthrough curve for chlorine at influent concentration $1.41 \times 10^{-5}\text{ mol/L}$ (1 ppm) onto RS-RH5%.

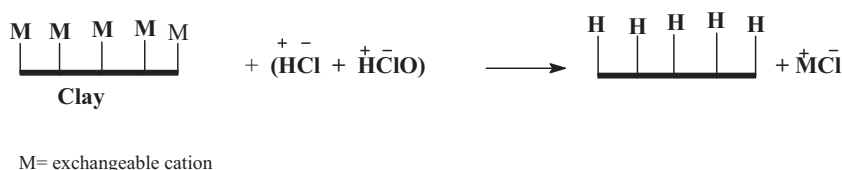


Figure 10 Schematic representation of cation exchange onto the clay surface.

fresh adsorbent at $C_o = 30$ ppm, indicating the stability and reusability of the ceramic adsorbent for several times.

3.4.3. Pb^{2+} and Ni^{2+} – Adsorption

Removal of the metals Ni(II) and Pb(II) (each studied individually) was assessed under dynamic conditions as explained before. The divalent metal concentration in the column influent (C_o) was fixed at 1.7×10^{-4} mol/L (corresponding to 10 ppm of Ni^{2+} and 35.2 ppm of Pb^{2+}). Fig. 8 depicts the breakthrough curve of the two divalent metals at room temperature onto the RS-RH5% surface. The higher value Q_{total} obtained was for the adsorption of 352.1 μmol Ni(II), while the adsorbed amount of Pb(II) was 316.3 μmol . The adsorption depends on the characteristics of the adsorbent and the adsorbate. These trends in the sorption may be explained on the basis of the ionic radius of the metal ions. The ionic radii of the metal ions are Ni^{2+} (0.83 Å) and Pb^{2+} (1.2 Å). It has been noted that the smaller the ionic diameter, the higher the adsorption rate [24]. Thus, from our study, Ni (II) ion which has smaller ionic radius had higher adsorption capacity. Therefore, the trend of ionic radii is in opposite direction to the trend of adsorption capacity.

Another factor that affects the adsorption affinity is the hydration energies of ions (ΔH_{hyd}). For Ni^{2+} cation, ΔH_{hyd} is $-2106 \text{ kJ mol}^{-1}$ and for Pb^{2+} is $-1480 \text{ kJ mol}^{-1}$. Therefore, Pb^{2+} cations are more hydrolysable, viz., has more tendency to be in aqueous medium and lower adsorption. Simply, the previous two factors are a direct application of Coulomb's law that describes force interacting between static electrically charged particles.

3.4.4. Adsorption of chlorine from aqueous medium

Fig. 9 shows the breakthrough curve of Cl_2 onto RS-RH5% at room temperature and influent concentration of 1.41×10^{-5} mol (1 ppm). Solution of chlorine in water contains chlorine (Cl_2), hydrochloric acid, and hypochlorous acid:



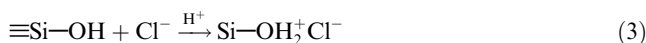
At the low concentrations, sorption rate is controlled by the cation exchange capacity [25] (see Fig. 10). During the adsorption process, the equilibrium of the above equation is shifted to right due to the sorption of components of right handside. The calculated amount of sorbed chlorine (numerically equals to the area under the curve) is 363.07 (see Fig. 9).

To verify this assumption, the sorption of chlorine solution in de-ionized water at initial concentration of 4.225×10^{-5} mol/L (3 ppm) was studied under the same conditions where the total chlorides in influent and in effluent were estimated through the comparison of free chlorine and chlorides (chlorides was estimated using standard 0.0141N silver nitrate and micro-pipette). The result shows that the sorbed amount of Cl_2 , the difference between the amount of chloride ions in

effluent and in influent and CEC of the adsorbent are almost equivalent:

$$[\text{Cl}_2]_{\text{sor}} \cong [\text{Cl}^-]_{\text{eff}} - [\text{Cl}^-]_{\text{inf}} \cong \text{CEC} = 12.5 \text{ mEq}/100 \text{ g} \quad (2)$$

Also, the interaction with the available silanol groups may be possible:



It is observed that the curve does not take the normal S-shape. This attributed to the low concentration of influent (1 ppm) and the kinetics of the sorption through ion exchange [17]. It is important to note that, at low concentrations in aqueous solutions, even in the case of physisorption, the adsorption is monolayer on the walls of the pores and not fill these pores as opposed to adsorption from the gaseous phase [26]. This means that the adsorption capacity of RS-RH5% for Cl_2 gas will be increased.

4. Conclusion

A novel cheap mesoporous adsorbent has been successfully prepared from wastes through the templating of water treatment sludge with rice husk. The obtained adsorbent has shown high adsorption capacity in removal of rosaniline dye and metallic cations from aqueous medium while the removal of chlorine is controlled by cation exchange capacity of the adsorbent. The reusability test has shown the ease desorption of dye with slightly alkaline water indicating the stability and reusability of the ceramic adsorbent for several times. These results indicate that a new inexpensive, reusable and mesoporous adsorbent has been prepared from renewable wastes.

References

- [1] S.K. Kansal, M. Singh, D. Sud, *Photodegradation* 16 (2006) 117–127.
- [2] M.S. Khehra, H.S. Saini, D.K. Sharma, et al, *Dyes Pigments* 70 (2006) 1–7.
- [3] M.A.M. Salleh, D.K. Mahmoud, W.A. Karim, A. Idris, *Desalination* 280 (2011) 1–13.
- [4] G. Crini, *Bioresour. Technol.* 97 (2006) 1061–1085.
- [5] V.K. Gupta, Suhas, *J. Environ. Manage.* 90 (2009) 2313–2342.
- [6] A. Demirbas, *J. Hazard. Mater.* 167 (2009) 1–9.
- [7] C. Wu, C. Lin, R. Chen, *J. Environ. Sci. Health A* 39 (2004) 717–728.
- [8] M. Kyncl, *GeoSci. Eng.* 1 (2008) 11–22.
- [9] G. Yushin, E.N. Hoffman, M.W. Barsoum, Y. Gogotsi, C.A. Howell, S.R. Sandeman, *Biomaterials* 27 (2006) 5755–5762.
- [10] S. Lei, J.I. Miyamoto, H. Kanoh, Y. Nakahigashi, K. Kaneko, *Carbon* 44 (2006) 1884–1890.
- [11] Y. Tao, H. Kanoh, L. Abrams, K. Kaneko, *Chem. Rev.* 106 (2006) 896–910.
- [12] R.C. Reynolds, *Clays Clay Miner.* 40 (1992) 387–396.

- [13] R.K. Iler, *The Chemistry of Silica*, Wiley, New York, 1979.
- [14] L. Rodriguez-Gonzalez, F. Hermes, M. Bertmer, *Appl. Catal., A* 328 (2007) 174–182.
- [15] O. Allahdin, M. Wartel, P. Recourt, B. Revel, B. Ouddane, G. Billon, J. Mabingui, A. Boughriet, *Appl. Clay Sci.* 90 (2014) 141–149.
- [16] M.A. Al-Ghouti, M.A.M. Khraisheh, M.N. Ahmad, *J. Hazard. Mater.* 16 (2006) 45–65.
- [17] K. Vijayaraghavan, Y.S. Yun, *J. Biotechnol.* 26 (2008) 266–291.
- [18] R.S.R. Machado, M.G. Fonseca, L.N.H. Arakaki, J.G.P. Espinola, S.F. Oliveira, *Talanta* 63 (2004) 317–322.
- [19] A.E. Ahmed, F. Adam, *Microporous Mesoporous Mater.* 103 (2007) 284–295.
- [20] A.M. El-Shabiny, S.M. Hammad, I.A. Ibrahim, A.K. Ismail, *J. Therm. Anal.* 46 (1996) 1421–1435.
- [21] C. Jihane, K. Monia, R. Mahmoud, B. Amina, *Sci. World J.* (2012), <http://dx.doi.org/10.1100/2012/512454>.
- [22] H.G. Karge, J. Weitkamp (Eds.), *Molecular Sieves Science and Technology*, Springer, Heidelberg, 2008, pp. 5–28.
- [23] C.-Y. Chen, J.C. Chang, A.H. Chen, *J. Hazard. Mater.* 185 (1) (2011) 430–441.
- [24] M. Ahmedna, M.M. Johns, S.J. Clarke, W.E. Marshall, R.M. Rao, *J. Sci. Food Agric.* 75 (1997) 117–124.
- [25] H. Ciesielski, T. Sterckeman, M. Santerne, J.P. Willery, *Agron. EDP Sci.* 17 (1) (1997) 9–16.
- [26] P.M. José, L. Svetlana, *Recent Advances in Adsorption Processes for Environmental Protection and Security*, first ed. Kyiv, Ukraine, 2006.